Asian Journal of Chemistry; Vol. 32, No. 9 (2020), 2119-2124

ASIAN JOURNAL OF CHEMISTRY

https://doi.org/10.14233/ajchem.2020.22645

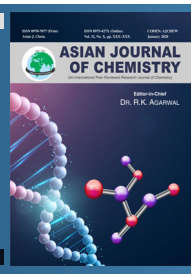

Synthesis and Characterization of SnO_2 and SnO_2/ZnO Nanoparticles by Electrochemical Method: Evaluation of their Performance in Photodegradation of Indigo Carmine Dye and Antibacterial Activity

K.P. SAMSKRUTHI[1,*], SANNAIAH ANANDA[1,*], M.B. NANDAPRAKASH[2] and K.S. CHANDRAKANTHA[3]

[1]Department of Studies in Chemistry, University of Mysore, Mysuru-570005, India
[2]Department of Physics, Yuvraja's College, Mysuru-570005, India
[3]Department of Materials Science, Mangalore University, Mangalagangothri D.K.-574199, India

*Corresponding authors: E-mail: samskruthi1994@gmail.com

Received: 21 January 2020; *Accepted*: 25 April 2020; *Published online*: 20 August 2020; AJC-19999

SnO_2 and SnO_2/ZnO nanoparticles were synthesized by the electrochemical method. The synthesized nanoparticles were characterized by XRD, UV-VIS, IR, FE-SEM and EDAX techniques. The X-ray diffraction revealed that the average crystalline size to be 79.78 and 22.84 nm. The band gap of SnO_2/ZnO nanoparticle from Tauc's plot was found to be 2.196 eV. The photocatalytic degradation of Indigo carmine dye follows the first order reaction. The antibacterial activity of SnO_2 and SnO_2/ZnO nanoparticles against *Staphylococcus aureus* and *Escherichia coli* was investigated.

Keywords: Nanoparticles, Electrochemical method, Photocatalytic activities, Indigo carmine, Biological activity.

INTRODUCTION

In recent years, nanotechnology has become one of the promising tools for scientific innovation. Metal nanoparticles have been great interest due to their distinctive features such as catalytic, optical, magnetic and electrical properties [1,2]. Catalysis using metal oxide nanoparticles having great importance and intensive research is being carrying out to ensure the biological activity. Nowadays photocatalysis has become more important since it has great potential to contribute towards the environment [3]. Studies have highlighted that ZnO exhibits better efficiency than TiO_2 for removing organic compounds in water-bodies [4]. ZnO is known to be one kind of the important photocatalyst because of its low price, high photocatalytic activity and nontoxicity, that has attracted a great deal of attention with respect to the degradation of various pollutant due to its high photosensitivity and stability[5].

Tin oxide (SnO_2) is a very unique material with its important properties such as low operating properties, high thermal stability and high degree of transparency in visible region of spectrum. It is an important n-type semiconductor with wide band energy (3.6-3.8eV) [6-8] and doping metal ions into ZnO can influence the performance of these photocatalysts. The largest enhancement of photoactivity through doping can be found in nano-sized particles [9]. Different methods have been used in the literature for the synthesis of SnO_2/ZnO or other metal oxides such as hydrothermal synthesis [10], sol-gel synthesis [11], microemulsion synthesis [12], combustion assisted facile green synthesis [13] and flame-spray pyrolysis (FSP) [14]. Electrochemical method is preferred method, which is simple, reliable and inexpensive method. In this article, synthesized SnO_2/ZnO nanoparticle enhance the photocatalytic activity of tin observed as the wide band gap of SnO_2 decreased from 3.6 eV to 2.916 eV in SnO_2/ZnO [15].

EXPERIMENTAL

All chemicals used were of analytical grades of purity, tin, zinc metals and sodium bicarbonate were purchased from Alfa-Aesar and Indigo carmine dye from Merck. All solutions were prepared in double-distilled water. Optical absorption spectra were recorded at room temperature on JASCO- UV VIS spectrophotometer. The crystallographic interpretations were performed by X-ray diffractometer (Rigaku miniflex II

desktop X-ray diffractometer) using Cu*K*α wavelength (λ = 1.54 Å). The morphological feature of the semiconductor was observed by scanning electron microscopy (Zeiss Evo LS15). The elemental analysis of nanoparticles was confirmed from Energy dispersive X-ray analysis (EDAX), recorded on HITACHI S-3400N Japan.

Electrochemical synthesis of SnO_2 and SnO_2/ZnO nanoparticles: SnO_2 and SnO_2/ZnO nanoparticles were synthesized by electrochemical method. For the synthesis of SnO_2 nanoparticles, tin metal wire was used as anode whereas platinum electrode as cathode. The experiment was run for 3 h with continuous stirring (20 mA, 16 V); the anodic dissolution of Sn to give Sn(IV) ions, which were electrochemically reacted with aqueous $NaHCO_3$ (5%) to form Sn(IV) oxides/hydroxides as shown in **Scheme-I**.

$$Sn \longrightarrow Sn^{4+} + 4e^-$$

$$2H_2O \longrightarrow 4H^+ + O_2 + 4e^-$$

$$Sn^{4+} + O_2 + 4e^- \longrightarrow SnO_2$$

Scheme-I: Synthesis of SnO_2 nanoparticles

Similarly for the synthesis of SnO_2/ZnO nanoparticles, tin and zinc metal wires were used as anode and platinum electrode as cathode. The experiment was run for 3 h with continuous stirring (20 mA, 16 V); the anodic dissolution of Zn and Sn to give Zn(II) and Sn(IV) ions which were electrochemically reacted with aqueous $NaHCO_3$ (5%) to form Sn(IV) and Zn(II) oxides/hydroxides (**Scheme-II**). The solid obtained was washed with deionized water till complete removal of unreacted $NaHCO_3$. The solid was then centrifuged and calcined for 2 h at 700 ºC for dehydration and for the removal of hydroxides to get SnO_2 and SnO_2/ZnO [16]. The rate of electrochemical reaction is not same for all the metals, as the redox potentials of zinc and tin metals are different. The rate of dissolution for Zn (-0.7618V) is faster than Sn (-0.13V) so that higher portion of Zn(II) or ZnO is formed than Sn(IV) or SnO_2 in SnO_2/ZnO nanoparticles. The electrochemical reaction takes place according to the following mechanism (**Scheme-II**).

$$Zn \rightleftharpoons Zn^{2+} + 2e^-$$

$$2NaHCO_3 + 2e^- \rightleftharpoons 2CO_2 + 2Na^+ + 2OH^-$$

$$Zn^{2+} + 2OH^- \rightleftharpoons Zn(OH)_2$$

$$Zn(OH)_2 \rightleftharpoons ZnO + H_2O$$

$$Zn + 2NaHCO_3 \rightleftharpoons ZnO + 2CO_2 + 2Na + H_2O$$

$$\text{In general, } M + NaHCO_3 \rightleftharpoons MO + CO_2 + Na + H_2O$$

$$\text{The overall reaction is, } Zn \xrightarrow[NaHCO_3]{Sn} SnO_2/ZnO \text{ nanoparticles}$$

Scheme-II: Synthesis of SnO_2/ZnO nanoparticles

Determination of photocatalytic activities: Indigo caramine dye solution was prepared by dissolving 4.66 g/100 mL in distilled water. This solution was then used as a test contaminant for investigating photocatalytic activities of synthesized SnO_2 and SnO_2/ZnO nanoparticles. The evaluation was carried out both under ultraviolet light and sunlight in order to investigate the efficiency of SnO_2 and SnO_2/ZnO nanoparticles. Chemical oxygen demand (COD) was estimated before and after treatment using dichromate oxidation method [17]. An increase in percent transmission and decrease in COD (mg/L) of the dye solution with colour removal was observed to be more in SnO_2/ZnO compared to SnO_2 nanoparticle.

Antibacterial assay: The antibacterial susceptibility of SnO_2 and SnO_2/ZnO was evaluated by using the disc diffusion Kirby-Bauer method in Mueller-Hinton agar plate. A 20 mL of sterilized and molten Mueller-Hinton agar media was poured in to the sterilized petri plates. The reference bacterial strains Gram-positive *Staphylococcus aureus* (MTCC 7443) and Gram-negative *Escherichia coli* (MTCC 40) obtained from Microbial Typing Culture Collection (MTCC), Chandigarh, India were cultured overnight at 37 ºC in Mueller-Hinton agar and adjusted to a final density of 107 CFU/mL by 0.5 McFarland standards. 100 µL of the pathogenic bacteria cultures were transferred onto plate and made culture lawn. The SnO_2 and SnO_2/ZnO were loaded into 6 mm sterile discs and placed on the culture plates and incubated at 37 ºC for 24 h. The comparative stability of discs containing gentamycin was made. By measuring the diameter of the ZOI formed around the disc, the antibacterial efficacy of SnO_2 and SnO_2/ZnO was determined.

RESULTS AND DISCUSSION

SEM analysis: The surface morphology of SnO_2 and SnO_2 /ZnO nanoparticles were investigated by SEM. The SEM morphology (Fig. 1) revealed that sample consist of aggregation of particles with cubic and monoclinic crystal like structure. The EDAX confirms the presence of Sn, Zn and O in the synthesized SnO_2 and SnO_2/ZnO nanoparticles (Fig. 2).

XRD analysis: The XRD patterns of SnO_2 and SnO_2/ZnO nanoparticles (Fig. 3) demonstrated that the (hkl) values according to Treor programming (IUCR) of the peaks at 2θ values of 16.14º, 18.77º, 32.82º, 34.21º, 39.22º, 55.87º and 57.65º can be associated with (111), (200), (222), (320), (410), (441) and (531), respectively. Meanwhile, the XRD results revealed that SnO_2 nanoparticles possess cubic crystal structure with lattice constants $a = b = c = 9.449$ Å, $\alpha = \beta = \gamma = 90º$ and with the average crystallite size of 79.78 nm and % strain was found to be 0.26. The XRD pattern of SnO_2/ZnO nanoparticles demonstrated that the peaks at 2θ values 16.07º, 31.69º, 32.81º, 34.24º, 36.17º, 39.31º, 47.40º, 55.72º, 56.72º, 57.56º, 60.50º and 67.81º can be associated with (200), (102), (102), (202), (120), (121), (402), (303), (230), (422), (023) and (114), respectively. The XRD results revealed that SnO_2/ZnO nanoparticles possess monoclinic crystal structure with lattice constants $a = 11.005$ Å, $b = 5.094$ Å, $c = 5.748$ Å, $\alpha = \gamma = 90º$ $\beta = 93.99º$ ($\alpha = \gamma = 90º \neq \beta$) and with the average crystallite size of 22.84 nm and % strain was found to be 0.22. The average crystallite size was calculated using Debye-Scherrer's equation [16].

FT-IR analysis: Fig. 4 represents the IR spectrum of SnO_2 /ZnO nanoparticles. The IR spectra indicate that the absorptions at 3446 cm^{-1} are evidently related to the presence of hydroxyl

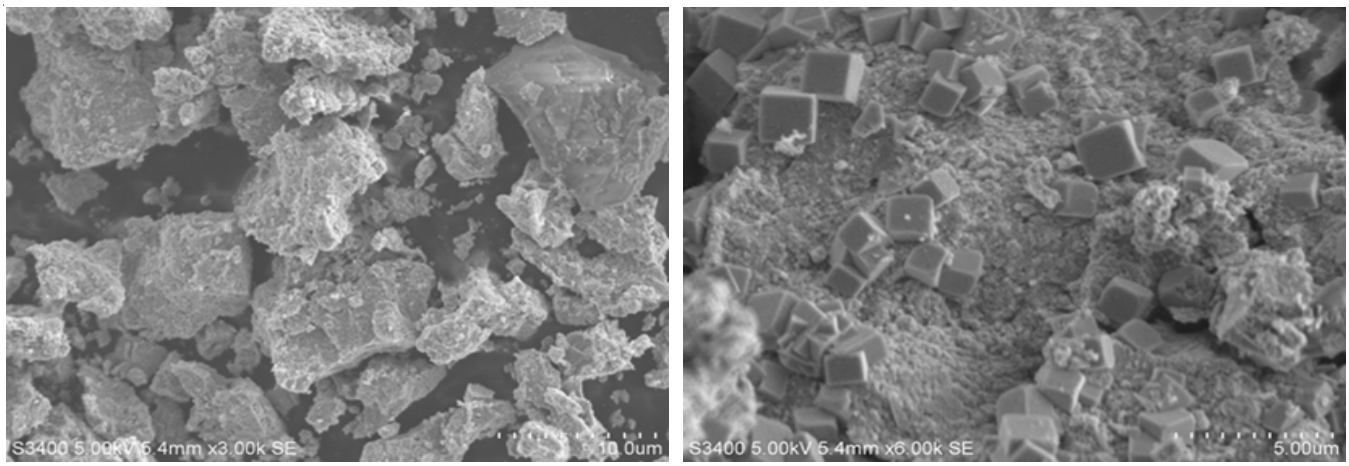

Fig. 1. SEM images of synthesized SnO_2 and SnO_2/ZnO nanoparticles

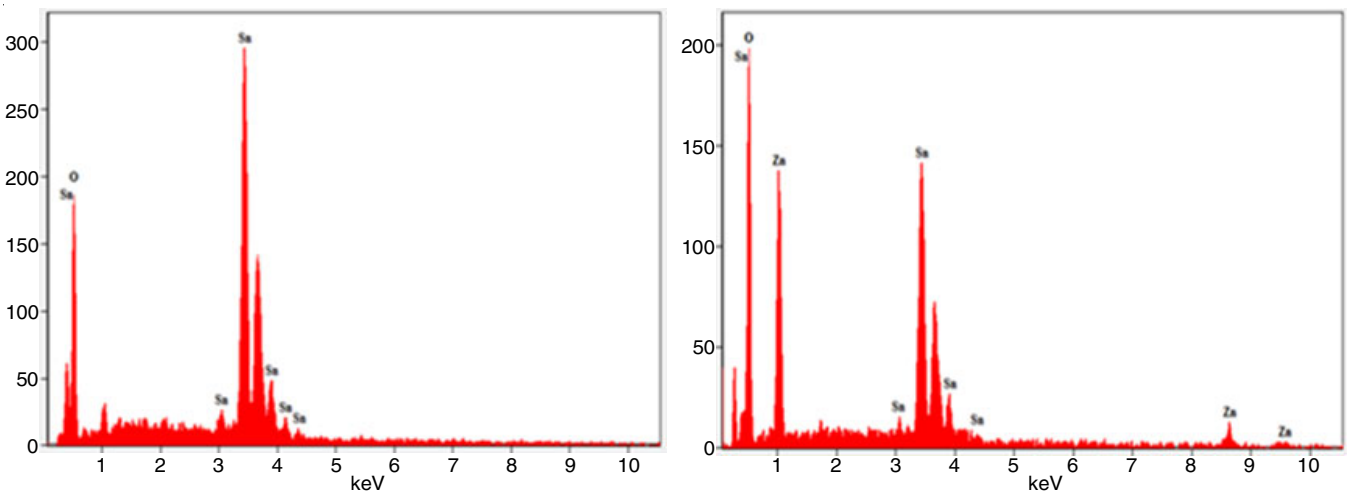

Fig. 2. EDAX of SnO_2 and SnO_2/ZnO nanoparticles

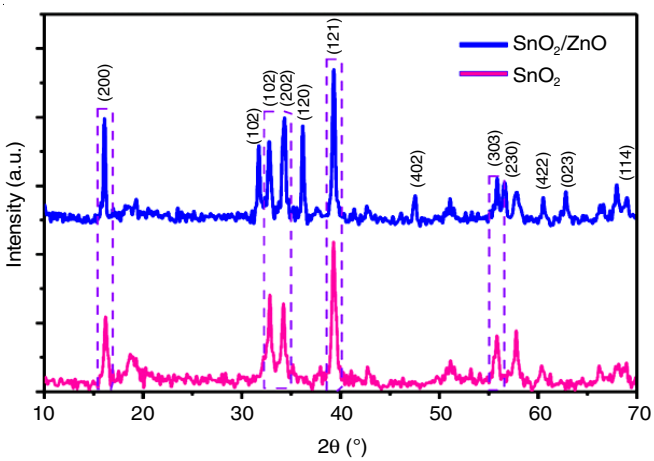

Fig. 3. XRD patterns of SnO_2 and SnO_2/ZnO nanoparticles

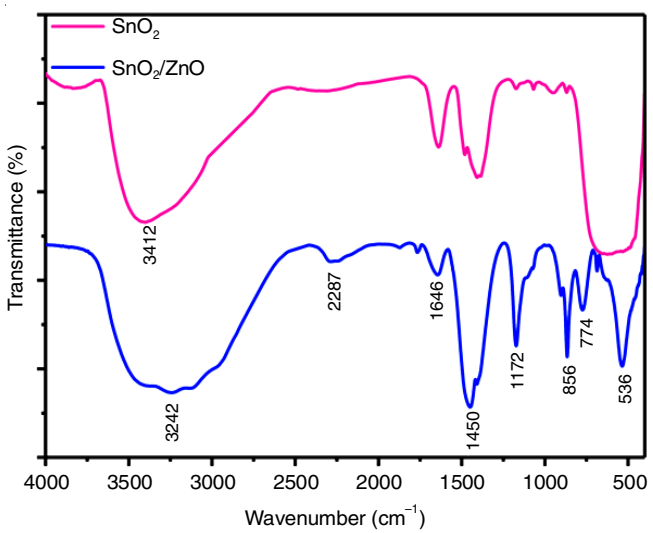

Fig. 4. FTIR spectra of SnO_2 and SnO_2/ZnO nanoparticles

groups of water molecules [18] on the outer surface of SnO_2 nanoparticles. A peaks at 1172 and 856 cm^{-1} correspond to Sn-O bending and stretching vibration. A peak at 1439 cm^{-1} indicates the formation of ZnO [19,20].

UV-visible analysis: UV-visible spectrum of SnO_2/ZnO over the range of 300-600 nm showed that the synthesized nanoparticles are photoactive under visible light irradiation. The band gap of SnO_2/ZnO was calculated using Tauc′s plot (Fig. 5). For a semiconductor sample, it is possible to determine the optical absorption near the band edge by the equation, $\alpha h\nu = A(h\nu - E_g)^{n/2}$ where α, h, ν, E_g and A are absorption coefficients, Plank′s constant, radiation frequency, band gap

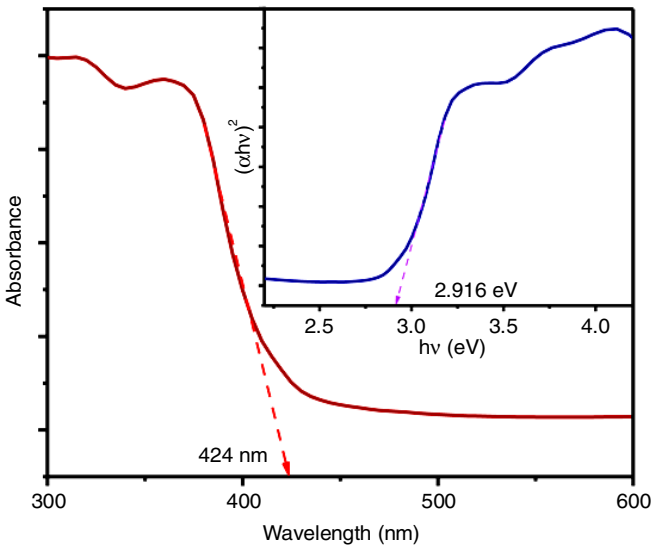

Fig. 5. UV spectra of SnO_2/ZnO nanoparticles

and a constant, respectively. The n value decides the characteristics of transition in a semiconductor being 1 or 4, respectively, for a direct or an indirect semiconductor. In order to get an accurate value of the band gap of solids, it is neccesary to construct a $(\alpha h\nu)^{1/2}$ *versus* hν also called Tauc plot [21]. From the optical absorption spectra, it is clear that synthesized SnO_2/ZnO nanoparticle has showed the maximum intensity peak at 484 nm. The band gap of the sample is calculated using Tauc plot and found to be 2.196 eV.

Determination of photocatalytic activities: Photodegradation assisted by semiconductor depends on various parameters like nature and concentration of the organic substrates, concentration and type of semiconductor, light source and intensity, pH, temperature, *etc*. [20]. Photodegradation experiments were carried out using different concentrations of Indigo carmine dye as substrate and different concentration of SnO_2/ZnO as catalyst. A calculated quantity of catalyst was added to a dye solution. Stirred in the dark to establish adsorption/desorption equilibrium between the dye and nanoparticle molecules and then illuminated under 8 W UV source to induce the photochemical reaction. Aliquots were taken at an interval of 2 min to determine the change of %T using Elico SL 171 (g%) was calculated was follows [22]:

$$\text{Photodegradation efficiency} = \frac{\text{Initial COD} - \text{Final COD}}{\text{Initial COD}} \times 100$$

Photodegradation kinetics and COD measurements

Effect of catalyst loading: Table-1 shows the rate constants of degradation with respect to different concentration of catalyst keeping dye concentration constant *i.e.* 4×10^{-4} M. Several studies have indicated that the photocatalytic rate initially increases with catalyst loading and then decreases at high values because of light scattering and screening effects [23]. The experiments were performed by taking different amount of catalyst varying from 10, 20, 30 and 50 mg keeping dye concentration constant in order to study the effect of catalyst loading. The study showed that an increase in catalyst loading up to 50 mg increased the dye removal efficiency. Further increase in catalyst above 50 mg decreased the photoactivity of catalyst due to aggregation of SnO_2/ZnO nanoparticles at higher concentration causing a decrease in the number of active sites on catalyst surface and increase in the light scattering of SnO_2/ZnO nanoparticles at high concentration [17]. This tends to decrease the passage of light through the sample. Further, the present study indicates from economic point of view, the optimized photocatalyst loading was 30 mg in 20 mL of dye solution. Rate of degradation is slow with SnO_2 compared to SnO_2/ZnO because the band gap of SnO_2 decreased from 3.6 eV to 2.916 eV in SnO_2/ZnO nanoparticles.

Effect of dye concentration: To know the optimum dye concentration, degradation is carried out in different concentration of dye. As the initial concentration of dye increases, the degradation efficiency reduces (Table-2). The possible reason is that as initial concentration of dye is increased; more dye molecule or abundant supply of dye molecules may act as filter for the incident light, preventing a sufficient intensity of light from reaching the dye molecule in the bulk solution and pathlength of the photons entering the solution is increased thereby fewer photons reached the catalyst surface [22].

Effect of pH: The pH of solution was adjusted by adding 0.01 M HCl solution and 0.01 M NaOH. The effect of pH was studied at pH 4.0, 6.0, 8.0 and pH 10.0 by keeping all other experimental conditions constant. From the results, it is observed that the rate of photodegradation increases from pH 4.0 to pH 8, the rate of degradation increases with increasing pH but at pH 10 rate of degradation decreases. Also, the amount of catalyst recovered after the experiment was lowered at lower pH because of the dissolution of semiconductor oxides at very low pH values. The optimum pH selected is 8 at which photodegradation is high (Table-3).

TABLE-1
EFFECT OF CATALYST AMOUNT OF ON THE RATE OF PHOTODEGRADATION OF INDIGO CARMINE DYE

Amount of catalyst (mg)	k (s^{-1})	Time taken for complete degradation	COD		Degradation efficiency (%)
			Before degradation	After degradation	
SnO_2/ZnO 10	1.9×10^{-4}	120	510	38	92.5
20	2.5×10^{-4}	100	510	26	95.0
30	2.6×10^{-4}	90	510	22	95.6
50	3.1×10^{-4}	80	510	18	96.5
SnO_2 10	0.6×10^{-4}	340	510	42	91.8
20	0.7×10^{-4}	300	510	39	92.4
30	1.2×10^{-4}	180	510	32	93.7
50	1.7×10^{-4}	140	510	21	95.8

TABLE-2
EFFECT OF CONCENTRATION OF INDIGO CARMINE DYE ON THE RATE OF PHOTODEGRADATION

Concentration of dye (10^{-5} M)	k (s^{-1})	Time taken for complete degradation	COD		Degradation efficiency (%)
			Before degradation	After degradation	
SnO_2/ZnO 1	2.8×10^{-4}	20	254	12	95.3
2	2.7×10^{-4}	30	368	19	94.8
3	2.6×10^{-4}	70	448	27	94.0
4	2.4×10^{-4}	90	496	38	92.3
5	2.3×10^{-4}	120	672	55	91.8
SnO_2 1	0.92×10^{-4}	80	254	19	92.5
2	0.8×10^{-4}	100	368	29	92.1
3	0.73×10^{-4}	140	448	37	91.7
4	0.65×10^{-4}	180	496	45	90.9
5	0.61×10^{-4}	220	672	63	90.6

TABLE-3
EFFECT OF pH ON THE RATE OF PHOTODEGRADATION OF INDIGO CARMINE DYE

pH	k (s^{-1})	Time taken for complete degradation	COD		Degradation efficiency (%)
			Before degradation	After degradation	
SnO_2/ZnO 4	1.8×10^{-4}	100	510	39	92.4
6	2.5×10^{-4}	80	510	35	93.1
8	2.8×10^{-4}	60	510	22	95.6
10	1.9×10^{-4}	90	510	37	92.7
SnO_2 4	1.03×10^{-4}	200	510	43	91.5
6	0.84×10^{-4}	180	510	36	92.9
8	1.34×10^{-4}	140	510	28	94.5
10	1.19×10^{-4}	160	510	41	91.9

Effect of catalyst in sunlight: The photodegradation rate with UV light was compared with the sunlight. It is observed that the photodegradation rate is fast in UV light than in sunlight for prepared photocatalyst SnO_2 and SnO_2/ZnO nanoparticles. It is noticed that the photodegradation rate was increased in sunlight for prepared SnO_2/ZnO than SnO_2. This is due to the combination of SnO_2 and ZnO in SnO_2/ZnO nanoparticles caused an decrease in the band gap of SnO_2 from 3.6 eV to 2.916 eV indicating that these semiconductor nanoparticles absorb sunlight. This can consequently activate these modified metal oxide photocatalysts upon sunlight irradiation (Table-4).

Reusability of photocatalyst: The possibility of reusing the photocatalyst was examined to see the cost effectiveness of the method. After the degradation of dye, the dye solution was kept standing for 12 h and then the supernatant was decanted. The photocatalyst was then thoroughly washed with double distilled water and reused for degradation with a fresh of dye solution. It was observed that the photocatalytic efficiency was slightly decreased to approximately 85% for the use of second time. The COD for washings of photocatalysts collected showed very lower values (~300 mg/L) indicating adsorption and photodegradation. Further use of the catalyst showed lesser efficiency.

Antibacterial assay: The antibacterial susceptibility of SnO_2 and SnO_2/ZnO was investigated by zone of inhibition by Kirby-Bauer disc diffusion method. Disposable plates inoculated with the Gram-positive and Gram-negative bacteria, such as *Staphylococcus aureus* and *Escherichia coli*. On the basis of the results obtained from microbiological studies (Table-5) the materials may be used as an antibacterial and antifungal agent.

Conclusion

In the present work, SnO_2 and SnO_2/ZnO nanoparticles are synthesized by electrochemical method an eco-friendly method. The photodegradation by this semiconductor offers a

TABLE-4
EFFECT OF SUNLIGHT ON THE RATE OF PHOTODEGRADATION OF INDIGO CARMINE DYE

Nanoparticle	k (s^{-1})	Time taken for complete degradation	COD		Degradation efficiency (%)
			Before degradation	After degradation	
SnO_2/ZnO	1.84×10^{-4}	120	507	32	93.7
SnO_2	1.18×10^{-4}	180	492	41	91.6

TABLE-5
ANTIBACTERIAL EFFECT OF SnO_2 AND SnO_2/ZnO AGAINST BACTERIAL STRAIN

Test bacteria	SnO_2	SnO_2/ZnO	Positive control [gentamycin (10 mcg)]
Staphylococcus aureus MTCC 7443	15.01 ± 0.19	18.01 ± 0.53	31.02 ± 0.25
Escherichia coli MTCC 40	20.01 ± 0.84	29.01 ± 0.34	30.31 ± 0.08

Note: Values are the mean ± SE of triplicate experiments.

green technology for the removal of hazardous components (organic dyes) present in wastewater and industrial effluents. Kinetics of photodegradation of Indigo carmine suggested that disappearance of Indigo carmine dye follows the first order kinetics and nanoparticles can be regenerated and reused with slightly lesser efficiency. The complete degradation reaction was confirmed by conducting COD experiments. The COD values revealed that 95% of the dye had been degraded. The synthesized nanoparticles showed a appreciably good inactivation of different strains of bacteria.

ACKNOWLEDGEMENTS

This work has been supported by University of Mysore, Mysuru and the authors acknowledge UGC-BSR and DST-PURSE Program, New Delhi, India.

CONFLICT OF INTEREST

The authors declare that there is no conflict of interests regarding the publication of this article.

REFERENCES

1. S.K. Sahoo, S. Parveen and J.J. Panda, *Nanomed.: Nanotechnol. Biol. Med.*, **3**, 20 (2007); https://doi.org/10.1016/j.nano.2006.11.008
2. I. Khan, K. Saeed and I. Khan, *Arabian J. Chem.*, **12**, 908 (2019); https://doi.org/10.1016/j.arabjc.2017.05.011
3. A Ghaderi, S Abbasi and F Farahbod, *Iran. J. Chem. Eng.*, **12**, 96 (2015).
4. Sowbhagya and S. Ananda, *Am. Chem. Sci. J.*, **4**, 616 (2014); https://doi.org/10.9734/ACSJ/2014/8748
5. Rakesh, S. Ananda, N.M.M. Gowda and K.R. Raksha, *Adv. Nanopart.*, **3**, 133 (2014); https://doi.org/10.4236/anp.2014.34018
6. H.-C. Chiu and C.-S. Yeh, *J. Phys. Chem. C*, **111**, 7256 (2007); https://doi.org/10.1021/jp0688355
7. M.A. Qamar, S. Shahid, S.A. Khar, S. Zaman and M.N. Sarwar, *Digest J. Nanomater. Biostuct.*, **12**, 1127 (2017).
8. M.A.M. Akhir, K. Mohamed, H.L. Lee and S.A. Rezan, *Procedia Chem.*, **19**, 993 (2016); https://doi.org/10.1016/j.proche.2016.03.148
9. P.A. Tran and T.J. Webster, *Int. J. Nanomedicine*, **6**, 1553 (2011); https://doi.org/10.2147/IJN.S21729
10. P.M. Aneesh, K.A. Vanaja and M.K. Jayaraj, *Nanophot. Mater. IV*, **6639**, 66390J (2007); https://doi.org/10.1117/12.730364
11. J. El Ghoul, M. Kraini and L. El Mir, *J. Mater. Sci. Mater. Electron.*, (2015); https://doi.org/10.1007/s10854-015-2722-z
12. C. Tojo, M. Dios and F. Barroso, *Materials*, **4**, 55 (2011); https://doi.org/10.3390/ma4010055
13. G.K. Prashanth, P.A. Prashanth, M. Gadewar, B.M. Nagabhushana, U. Bora, S. Ananda, G.M. Krishnaiah and H.M. Sathyananda, *Karbala Int. J. Modern Sci.*, **1**, 67 (2015); https://doi.org/10.1016/j.kijoms.2015.10.007
14. M. Yurddaskal, S. Yildirim, T. Dikici, M. Yurddaskal, M. Erol, I. Aritman and E. Celik, *J. Turk. Chem. Soc.: Chem.*, **5A**, 15 (2017); https://doi.org/10.18596/jotcsa.370748
15. V. Kumar, K. Singh, J. Sharma, A. Kumar, A. Vij and A. Thakur, *J. Mater. Sci. Mater. Electron.*, **28**, 18849 (2017); https://doi.org/10.1007/s10854-017-7836-z
16. H.B. Uma, S. Ananda, R.R. Vittal and K.A. Zarasvand, *Modern Res. Catal.*, **6**, 30 (2017); https://doi.org/10.4236/mrc.2017.61003
17. H.C. Charan Kumar, R. Shilpa, V.R. Shankar Rai and S. Ananda, *J. Appl. Chem.*, **8**, 622 (2019).
18. S. Abbasi, S.M. Zebarjad, S.H. Noie Baghban and A. Youssefi, *Synth. React. Inorg. Met.-Org. Nano-Met. Chem.*, **45**, 1539 (2015); https://doi.org/10.1080/15533174.2013.862820
19. G.C. Lakshmi, S. Ananda, R. Somashekar and C. Ranganathaiah, *Int. J. Adv. Sci. Technol.*, **5**, 221 (2012).
20. K. Byrappa, A.K. Subramani, S. Ananda, K.M.L. Rai, R. Dinesh and M. Yoshimura, *Bull. Mater. Sci.*, **29**, 433 (2006); https://doi.org/10.1007/BF02914073
21. C. Belver, C. Adán and M. Fernández-García, *Catal. Today*, **143**, 274 (2009); https://doi.org/10.1016/j.cattod.2008.09.011
22. K.R. Raksha, S. Ananda and N.M. Madegowda, *J. Mol. Catal. Chem.*, **396**, 319 (2015); https://doi.org/10.1016/j.molcata.2014.10.005
23. K.R. Raksha and S. Ananda, *J. Appl. Chem.*, **3**, 397 (2014).